Theory and computer simulation for the cubatic phase of cut spheres

Peter D. Duncan,[1,*] Matthew Dennison,[2] Andrew J. Masters,[2] and Mark R. Wilson[1]
[1]*Department of Chemistry, University of Durham, South Road, Durham DH1 3LE, United Kingdom*
[2]*School of Chemical Engineering and Analytical Science, University of Manchester, P.O. Box 88, Sackville Street, Manchester M60 1QD, United Kingdom*
(Received 13 November 2008; published 4 March 2009)

The phase behavior of a system of hard-cut spheres has been studied using a high-order virial theory and by Monte Carlo simulation. The cut-sphere particles are disks of thickness L formed by symmetrically truncating the end caps of a sphere of diameter D. The virial theory predicts a stable nematic phase for aspect ratio $L/D=0.1$ and a stable cubatic phase for $L/D=0.15–0.3$. The virial series converges rapidly on the equation of state of the isotropic and nematic phases, while for the cubatic phase the convergence is slower, but still gives good agreement with the simulation at high order. It is found that a high-order expansion (up to B_8) is required to predict a stable cubatic phase for $L/D \geqslant 0.15$, indicating the importance of many-body interactions in stabilizing this phase. Previous simulation work on this system has focused on aspect ratios $L/D=0.1$, 0.2, and 0.3. We expand this to include also $L/D=0.15$ and 0.25, and we introduce a fourth-rank tensor to measure cubatic ordering. We have applied a multiparticle move which dramatically speeds the attainment of equilibrium in the nematic phase and therefore is of great benefit in the study of the isotropic-nematic phase transition. In agreement with the theory, our simulations confirm the stability of the nematic phase for $L/D=0.1$ and the stability of the cubatic phase over the nematic for $L/D=0.15–0.3$. There is, however, some doubt about the stability of the cubatic phase with respect to the columnar. We have shown that the cubatic phase found on compression at $L/D=0.1$ is definitely metastable, but the results for $L/D=0.2$ were less conclusive.

DOI: 10.1103/PhysRevE.79.031702 PACS number(s): 61.30.−v

I. INTRODUCTION

It is well known experimentally that disk-shaped as well as rod-shaped particles can form liquid-crystalline phases. In particular, discotic nematic and columnar phases have been observed. In simulations, there have been a variety of models proposed for discotic liquid crystals. Among the purely repulsive hard-particle models are infinitely thin disks [1] or hard ellipsoids [2]. In the latter case, both rod-shaped and discotic particles could be simulated by varying the aspect ratio. In both these hard-repulsive-particle systems, a nematic phase was observed, but no columnar phase. Columnar phases can be found in systems which include attractive interactions favoring the face-to-face stacking of disks—e.g., the discotic form of the Gay-Berne potential [3] or hard ellipsoids with additional attractive interactions [4]. Caprion *et al.* investigated the effect of shape and energy anisotropies in the Gay-Berne potential for discotic particles [5]. Another discotic model, similar to the Gay-Berne model was proposed by Zewdie [6]. The parameters can be tuned to favor different kinds of ordering—e.g., nematic or columnar. There have also been studies aimed more at simulating particular discotic molecules known to exhibit liquid crystalline phases—e.g., an atomistic study of hexabenzocoronene derivatives [7] or the proposal of a coarse-grained interaction potential for polyaromatic hydrocarbons based on density-functional-theory calculations [8].

One model without attractive interactions which nevertheless does exhibit a columnar phase is the system of hard-cut spheres—i.e., spheres of diameter D with their end caps symmetrically truncated to form disks of thickness L. The phase diagram was first mapped out by Veerman and Frenkel [9] using Monte Carlo simulations in the constant-NVT ensemble. In addition to the nematic and columnar mesophases, an interesting "cubatic" phase was reported. In this phase, the particles form short stacks of typically four or five particles with neighboring stacks tending to be perpendicular to one another. The particles thus align along three perpendicular axes giving a phase with cubic orientational symmetry.

A more recent study of the cut-sphere system focused on the effect of confinement on the isotropic-nematic phase transition [10], but did not investigate the cubatic phase. There have been two further papers which report some limited simulation results as part of larger studies. Zhang *et al.* [11] performed simulations of mixtures of colloidal platelets and nonadsorbing polymers, but also report some results for the pure cut-sphere system with aspect ratio $L/D=0.1$, and van der Beek *et al.* [12] obtained the equation of state for $L/D=1/15$ in support of their experimental work on colloidal platelets.

Consideration of the cubatic phase in cut spheres, where particles with aspect ratio $L/D=0.2$ form stacks of four or five particles, led Blaak *et al.* [13] to speculate whether a system of cylinders with a length to diameter ratio of 0.9 might also exhibit a similar cubatic phase. However, they did not find such a phase in their simulations.

Besides hard-cut spheres, the cubatic phase is also predicted theoretically to occur in some other systems. These include Onsager crosses [14] and tetrapods [15]. A cubatic phase has also been reported in simulations of hard cuboids [16,17]. This phase is slightly different in nature to that observed in the cut-sphere system. It is the axes of the particles

*P.D.Duncan@durham.ac.uk

themselves which align in a structure with cubic symmetry, rather than stacks of particles.

In two dimensions, the cut-disk system exhibits a phase analogous to the cubatic phase with perpendicular stacks of particles [18] and the hard-rectangle system exhibits a "tetratic" phase in which the particles align preferentially along two orthogonal directions, but with no translational order [19,20].

To our knowledge the cubatic phase has never been observed in the laboratory, although a method has recently been devised to make tetrapod-shaped nanocrystals [21]. This raises the possibility of observing the cubatic phase experimentally in colloidal suspensions of these particles.

In this paper, we reexamine the phase diagram of the hard-cut sphere system using a high-order virial theory and by Monte Carlo computer simulation. Veerman and Frenkel's earlier simulation study focused on aspect ratios $L/D=0.1$, 0.2, and 0.3. We extend this to include $L/D=0.15$ and 0.25. Our theory and simulations both find a stable nematic phase for $L/D=0.1$. For $L/D \geqslant 0.15$ there is no nematic phase, but instead we find a cubatic phase. A high-order virial expansion (up to B_8) was needed to predict the stability of the cubatic phase over the nematic, emphasizing the importance of many-body interactions in stabilising the cubatic phase. Previous studies of liquid-crystalline phases using the virial series have shown good convergence of the predicted equations of state for truncation at B_8-level theory [22,23]. Here, the virial equations of state show good agreement with the equations of state obtained in the simulations.

In our simulations, we identify the phases from snapshots and by using various pair distribution functions. We also introduce a fourth-rank tensor order parameter to measure cubatic order from which it is possible to obtain the cubatic axes. Our simulations confirm the stability of the cubatic phase relative to the nematic phase for $L/D \geqslant 0.15$, but it is less clear whether the cubatic is metastable with respect to the columnar phase. By performing long runs for $L/D=0.1$ at a single state point, we were able to demonstrate that the cubatic phase will convert into a columnar, showing that the cubatic phase is metastable in this case. The results were less conclusive in the $L/D=0.2$ case.

It was found that extremely long runs were required to equilibrate the ordered phases. In an attempt to alleviate this problem, we have implemented a multiparticle move due to Jaster [24] and show that it is very effective for the study of the isotropic-nematic phase transition.

II. SIMULATION DETAILS

Monte Carlo simulations were carried out on systems of 216, 512, or 1728 hard-cut spheres with aspect ratios $L/D=0.1$, 0.15, 0.2, 0.25, and 0.3 in the *NPT* ensemble. Details of the overlap criteria for cut spheres can be found in Ref. [25]. Volume moves were carried out after every cycle. We define a cycle as one attempted move per particle. In high-density ordered phases the structure may be incommensurate with the periodic boundary conditions if a cubic simulation cell is used. We therefore allowed the x, y, and z box lengths to vary independently in such cases.

For all values of L/D we have performed compression runs starting at low pressure in the isotropic phase and an expansion run starting from a close-packed solid configuration at high pressure. Expansion and compression runs were also performed starting from an equilibrated configuration at a state point in the nematic ($L/D=0.1$) or cubatic ($L/D \geqslant 0.15$) phase. Typical production runs were 2×10^5 Monte Carlo (MC) cycles in length after equilibration runs of comparable length, but in excess of 10^6 MC cycles were required for equilibration near phase transitions.

We use the following reduced units. The reduced density is defined as $\rho^*=\rho/\rho_{CP}$, where

$$\rho_{CP}=\frac{2(D/L)}{\sqrt{3-(L/D)^2}} \tag{1}$$

is the density of the close-packed solid structure. The reduced pressure is defined by $P^*=Pv_0/k_BT$, where v_0 is the volume of a particle:

$$v_0=\frac{\pi}{12}D^3\frac{L}{D}\left[3-\left(\frac{L}{D}\right)^2\right]. \tag{2}$$

A. Distribution functions

We have measured various pair correlation functions in order to probe the structure of the system. $g(r_\parallel)$ and $g(r_\perp)$ are useful in the columnar phase. Here $r_\parallel$ and $r_\perp$ are the distance in the direction parallel and perpendicular to the orientation of the particle at the origin, respectively. In the columnar phase, $g(r_\parallel)$ probes correlations along the columns and $g(r_\perp)$ describes the two-dimensional packing of the columns. $g_P(r_\perp)$ is like $g(r_\perp)$ except that we only consider particles which are within a distance of $L/2$ of the equatorial plane of the particle at the origin. The orientational correlation functions $g_l(r)$ are defined as $g_l(r)=\langle P_l(\cos\theta)\rangle$, where P_l is the lth Legendre polynomial and θ is the angle between a particle at the origin and a particle a distance r away.

B. Order parameters

As an order parameter in the nematic phase, we used the standard second-rank order tensor

$$S_{\alpha\beta}=u_\alpha u_\beta-\frac{1}{3}\delta_{\alpha\beta}, \tag{3}$$

where $\mathbf{u}$ is a unit vector normal to the cut sphere. We define an order parameter S_{nem} as the largest eigenvalue of this tensor.

To quantify cubatic order, we define the fourth-rank tensor

$$\begin{aligned}Q_{\alpha\beta\gamma\delta}=&\frac{35}{8}u_\alpha u_\beta u_\gamma u_\delta-\frac{5}{8}(u_\alpha u_\beta\delta_{\gamma\delta}+u_\alpha u_\gamma\delta_{\beta\delta}+u_\alpha u_\delta\delta_{\beta\gamma}\\&+u_\beta u_\gamma\delta_{\alpha\delta}+u_\beta u_\delta\delta_{\alpha\gamma}+u_\gamma u_\delta\delta_{\alpha\beta})\\&+\frac{1}{8}(\delta_{\alpha\beta}\delta_{\gamma\delta}+\delta_{\alpha\gamma}\delta_{\beta\delta}+\delta_{\alpha\delta}\delta_{\beta\gamma}).\end{aligned} \tag{4}$$

This is the fourth-rank irreducible tensor, closely related to the set of fourth-rank spherical harmonics. It is highly symmetric and has the following properties:

$$Q_{\alpha\beta\gamma\delta}\delta_{\gamma\delta}=0, \tag{5}$$

$$Q_{\alpha\beta\gamma\delta}u_\gamma u_\delta=0. \tag{6}$$

In a cubatic phase the average of Q is given by

$$\langle Q_{\alpha\beta\gamma\delta}\rangle=\frac{S_{\mathrm{cub}}}{3}\sum_{i=1}^{3}\left[\frac{35}{8}x_{i\alpha}x_{i\beta}x_{i\gamma}x_{i\delta}-\frac{5}{8}(x_{i\alpha}x_{i\beta}\delta_{\gamma\delta}+x_{i\alpha}x_{i\gamma}\delta_{\beta\delta}+x_{i\alpha}x_{i\delta}\delta_{\beta\gamma}+x_{i\beta}x_{i\gamma}\delta_{\alpha\delta}+x_{i\beta}x_{i\delta}\delta_{\alpha\gamma}+x_{i\gamma}x_{i\delta}\delta_{\alpha\beta})+\frac{1}{8}(\delta_{\alpha\beta}\delta_{\gamma\delta}+\delta_{\alpha\gamma}\delta_{\beta\delta}+\delta_{\alpha\delta}\delta_{\beta\gamma})\right], \tag{7}$$

where $\mathbf{x}_i$ is a unit vector along the ith Cartesian axis in the frame of the cubatic phase. For perfect cubatic ordering, with molecules pointing with probability $1/3$ along each of the three axes, $S_{\mathrm{cub}}=1$. Noting that

$$x_{i\alpha}x_{i\beta}=\delta_{\alpha\beta}, \tag{8}$$

with the summation convention employed over the index i, we can simplify the above expression, obtaining (with no summation over j),

$$\langle Q_{\alpha\beta\gamma\delta}\rangle x_{j\gamma}x_{j\delta}=\frac{7S_{\mathrm{cub}}}{8}\left(x_{j\alpha}x_{j\beta}-\frac{1}{3}\delta_{\alpha\beta}\right). \tag{9}$$

Since $\langle Q_{\alpha\beta\gamma\delta}\rangle\delta_{\gamma\delta}=0$, we have the following eigentensor equation:

$$\langle Q_{\alpha\beta\gamma\delta}\rangle\left(x_{j\gamma}x_{j\delta}-\frac{1}{3}\delta_{\gamma\delta}\right)=\frac{7S_{\mathrm{cub}}}{8}\left(x_{j\alpha}x_{j\beta}-\frac{1}{3}\delta_{\alpha\beta}\right) \tag{10}$$

or

$$\langle Q_{\alpha\beta\gamma\delta}\rangle S_{\gamma\delta}=\frac{7S_{\mathrm{cub}}}{8}S_{\alpha\beta}, \tag{11}$$

where we define a second-rank tensor S. For each of the five independent elements of the eigentensor, $(\alpha,\beta)=(x,x),(x,y),(x,z),(y,y),(y,z)$, we can explicitly write out Eq. (11). This gives us a set of five simultaneous equations, which can be written as an ordinary eigenvalue problem with maximum eigenvalue $7S_{\mathrm{cub}}/8$. From the eigenvector of this equation (with components $S_{xx},S_{xy},S_{xz},S_{yy},S_{zz}$) the full second-rank eigentensor can be reconstructed using the symmetries $S_{xy}=S_{yx}$, etc., and the fact that $S_{xx}+S_{yy}+S_{zz}=0$. Finally, the eigenvectors of S should give the three orthogonal cubatic axes.

In summary, to calculate the cubatic order parameter and axes in a simulation, the following steps should be performed. (i) Form $Q_{\alpha\beta\gamma\delta}$ using the orientations of the particles in the system. (ii) Set up the five simultaneous equations from the eigentensor equation [Eq. (11)]. (iii) Diagonalize this matrix. The cubatic order parameter can be obtained from the largest eigenvalue $7S_{\mathrm{cub}}/8$. (iv) Reconstruct S from the eigenvector of this last matrix. The eigenvectors of S give the cubatic axes.

III. VIRIAL THEORY

The Helmholtz energy A of N particles with volume V and temperature T may be written as

$$A=A_0+Nk_BT\left(\int f(\boldsymbol{u})\ln[4\pi f(\boldsymbol{u})]d\boldsymbol{u}-1+\ln\rho+\sum_{n=2}\frac{1}{n-1}B_n\rho^{n-1}\right), \tag{12}$$

where A_0 is an ideal gas contribution, related to rotational motion, B_n is the nth virial coefficient, $f(\mathbf{u})$ is the one-particle distribution function of particle orientation $\mathbf{u}$, and ρ is the particle number density N/V.

$f(\mathbf{u})$ is determined as the function that minimizes A, subject to the normalization condition

$$\int f(u)du=1. \tag{13}$$

At low densities, the only solution is $f(\mathbf{u})=\frac{1}{4\pi}$, which corresponds to the isotropic phase. At higher densities, other solutions also appear. To investigate nematic formation, Onsager assumed that $f(\mathbf{u})$ takes the form

$$f(\boldsymbol{u},\alpha)=(\alpha/4\pi\sinh(\alpha))\cosh(\alpha\cos\theta), \tag{14}$$

where α is a parameter describing the nematic ordering of the system about the director z and ranges from 0 for isotropic ordering $[f(\mathbf{u})=\frac{1}{4\pi}]$ to ∞ for "perfect" nematic ordering. θ is the angle that each particle makes with this director. The nematic virial coefficients are also dependent on $f(\mathbf{u})$. The expression for the second virial is given as

$$B_2(\alpha)=-\frac{1}{2V}\int\int\int\int f(\boldsymbol{u}_1)f(\boldsymbol{u}_2)f_{12}d\boldsymbol{u}_1d\boldsymbol{u}_2d\boldsymbol{r}_1d\boldsymbol{r}_2, \tag{15}$$

where f_{12} is the Mayer f bond between particles 1 and 2, which, for hard particles, is 0 when the particles are overlapping and -1 when they are not. The calculation of B_3 is more complex. The integral to be solved is

$$B_3(\alpha)=-\frac{1}{3V}\int\int\int\int\int\int f(\boldsymbol{u}_1)f(\boldsymbol{u}_2)f(\boldsymbol{u}_3)f_{12}f_{23}f_{31}\times d\boldsymbol{u}_1d\boldsymbol{u}_2d\boldsymbol{u}_3d\boldsymbol{r}_1d\boldsymbol{r}_2d\boldsymbol{r}_3. \tag{16}$$

The general integral for the nth virial coefficient is

$$B_n(\alpha)=\frac{1-n}{n!V}\int\cdots\int f(\boldsymbol{u}_1)\cdots f(\boldsymbol{u}_\mathbf{n})V_nd\boldsymbol{u}_1\cdots d\boldsymbol{u}_\mathbf{n}d\boldsymbol{r}_1\cdots\times d\boldsymbol{r}_\mathbf{n}, \tag{17}$$

where

$$V_n=\sum_{S_n}\prod_{i<j}^{n}f_{ij}. \tag{18}$$

Here, the sum over S_n represents the sum over all star diagrams with n points. The virials are calculated using a modified Ree-Hoover method [26]. Each virial coefficient is cal-

culated for various values of α, from isotropic to perfect nematic ordering. This gives us the virial coefficients as a function of α. The Helmholtz energy can be minimized with respect to α at a given ρ, thus giving the ordering of the system at that density. From the Helmholtz energy, the pressure and chemical potential of the system at a given density can now be calculated for the nematic phase. In the isotropic phase, the value of α is kept as 0. For coexistence, the following criteria must be satisfied:

$$\mu_N(\rho_{nem}) = \mu_I(\rho_{iso}) \tag{19}$$

and

$$P_N(\rho_{nem}) = P_I(\rho_{iso}). \tag{20}$$

This method can be adapted for the cubatic liquid-crystalline phase. The first step is to modify the one-particle distribution function to take the cubic orientational ordering of the cubatic phase into account. Modifying the Onsager trial function [Eq. (14)] gives

$$f(u) = f_x + f_y + f_z, \tag{21}$$

with

$$f_x = \left(\frac{\alpha}{12\pi \sinh(\alpha)}\right)\cosh(\alpha \sin\theta \cos\phi) \tag{22}$$

$$f_y = \left(\frac{\alpha}{12\pi \sinh(\alpha)}\right)\cosh(\alpha \sin\theta \sin\phi) \tag{23}$$

$$f_z = \left(\frac{\alpha}{12\pi \sinh(\alpha)}\right)\cosh(\alpha \cos\theta), \tag{24}$$

where ϕ is the angle that the particle director makes with the x-axis cubatic director. α now describes the cubatic ordering of the system. This is then used to calculate the virial coefficients, using Eq. (17). With the virials calculated and the distribution function known, the Helmholtz energy [Eq. (12)] can be minimized with respect to α to give the cubatic order of the system as a function of density. Again, from the Helmholtz free energy the chemical potential and pressure can be calculated and using the conditions

$$\mu_C(\rho_{cub}) = \mu_I(\rho_{iso}) \tag{25}$$

and

$$P_C(\rho_{cub}) = P_I(\rho_{iso}), \tag{26}$$

the coexistence densities of the isotropic and cubatic phases can be found. For the cubatic phase to be stable with respect to the nematic phase, the coexistence density must be lower than that for the nematic phase. We can also seek to locate any nematic-cubatic transitions using these methods. Simulation indicates, however, that this transition does not occur, so we concentrate here on isotropic–liquid-crystalline transitions.

While it is computationally convenient to assume a parametrized trial function for $f(\mathbf{u})$, one may ask how this assumption affects the quality of the predictions. We have therefore also expanded the first five orientational virial coefficients in a large orientational basis set and thus calculated a high quality $f(\mathbf{u})$. Our current results compare well with this more exact treatment. This issue will be discussed further in a future publication.

The virial expression used here provides no information about local, short-range positional order. By this, we mean the shell structure found in simple isotropic fluids and the small stack structures reported in the cubatic phase [9]. The effects of this local structure on thermodynamic properties are included in the various integrations required to calculate the virial coefficients. One can obtain structual information by, for example, calculating the virial expansion of the direct correlation function. Preliminary results are reported in [27].

IV. THEORETICAL RESULTS

Using the above method, values of B_2-B_8 were calculated for the isotropic, nematic, and cubatic phases. This then gave the equations of state for both the isotropic-nematic and isotropic-cubatic phase transitions at each virial level, for $L/D=0.1$, 0.15, 0.2, 0.25, and 0.3. These are compared in Fig. 1 with the equations of state obtained from simulation (Sec. V). The coexistence densities, pressures, and order parameters at coexistence are given in Table I.

For $L/D=0.1$, the nematic phase is predicted to be stable with respect to the cubatic phase. That is, the isotropic-nematic phase transition occurs at a lower density than the isotropic-cubatic phase transition. This is true for all levels of the virial theory. This is consistent with simulation results, where a nematic phase is formed from the isotropic phase. At the B_2-B_4 level, the cubatic transition is predicted at a much higher density than the nematic transition, and at the B_5-B_8 level, no stable cubatic transition is observed. The predicted coexistence densities for the isotropic-nematic phase transition converge fairly rapidly. From B_3-B_6 level theory, the coexistence densities are fairly consistent, with some fluctuation about the "true" values. From B_7-B_8 level theory, no stable transitions are observed, which could be due to the relatively low value of these virials for $L/D=0.1$, which means there is a large error in its calculation, and also due to the negative isotropic virial values for B_7 causing a fall in pressure at high density. The calculated equations of state also converge on the equation of state obtained by simulation, and the predictions are particularly good at lower densities, with some divergence at higher densities. This is to be expected, as the higher-order virials account for many-body effects, which become important at higher densities.

For $L/D=0.15-0.3$, the theory predicts a stable cubatic phase at high-order virial theory, consistent with simulation. At low-order theory, a nematic phase is predicted. For $L/D=0.15$, it is not until B_8 level theory that a cubatic phase is predicted. At B_2-B_4 level theory, the isotropic-cubatic phase transition is predicted at a much higher density than the isotropic-nematic phase transition. At the B_5-B_7 level, no stable cubatic phase is observed, and it is only at B_8 level theory that a cubatic phase is predicted that is stable with respect to the nematic phase. It can be seen in Fig. 1 that the B_8 level predicted equation of state seems to be reaching a plateau. For a truncated series, negative coefficients may lead

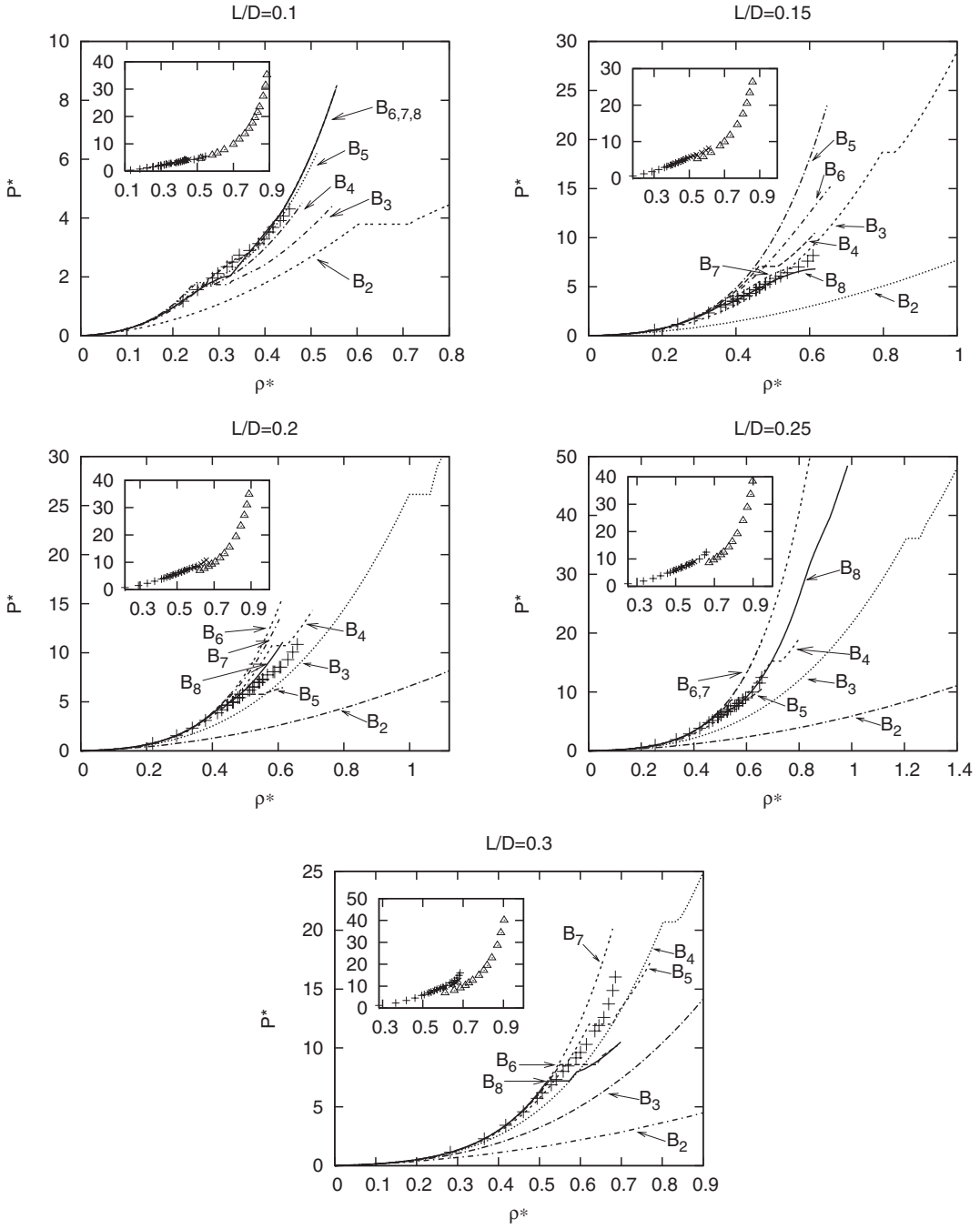

FIG. 1. Comparison of equations of state obtained from the virial expansion with those obtained by computer simulation. The insets show the equation of state from simulation over a wider density range: compression runs starting from isotropic phase (+), expansion and compression runs starting from a point in the nematic or cubatic phases (×), and expansion runs from the solid phase (triangles).

to a plateau, or even a negative value of $(\frac{\delta P}{\delta \rho})_T$. For a perfectly ordered cubatic phase, B_4 and B_5 are negative, while B_7 and B_8 are positive, leading to the observed behavior. For $L/D=0.2$ and 0.25, the behavior is similar, except that an isotropic-cubatic transition is observed at B_5 level theory, at a density just higher than the isotropic-nematic transition. Again, no isotropic-cubatic transition is observed at the B_6-B_7 level, and at B_8, a stable cubatic phase is predicted with respect to the nematic phase. Finally, at $L/D=0.3$, the nematic phase is predicted to be the stable phase at B_2-B_5 level theory, but at the B_6 level, the cubatic phase is predicted to be stable with respect to the nematic. The isotropic-cubatic transition is lost at the B_7 level, but at B_8, it is again observed to be stable with respect to the nematic phase. It can be seen from this that it is the high-order ($>B_6$) virial coefficients that stabilize the cubatic phase. As these high-order virial coefficients take many-body interactions into account, it is these many-body interactions that must stabilize the cubatic phase.

The convergence of the predicted coexistence densities for these particles is much less rapid for the cubatic phase than for the nematic phase predicted for $L/D=0.1$. This is

TABLE I. Coexistence data for the isotropic-nematic and isotropic-cubatic phase transitions at various levels of virial theory. P_N^* (P_C^*) is the pressure at the isotropic-nematic (isotropic-cubatic) phase transition, and ρ_I^* and ρ_N^* (ρ_C^*) are the densities of the coexisting isotropic and nematic (cubatic) phases, respectively.

			$L/D=0.1$			
Virial level	ρ_I^*	ρ_N^*	P_N^*	ρ_I^*	ρ_C^*	P_C^*
B_2	0.615	0.725	3.937	3.265	3.366	98.447
B_3	0.273	0.325	1.827	0.571	0.610	11.862
B_4	0.240	0.283	1.688	0.325	0.389	3.867
B_5	0.256	0.293	1.906	*	*	*
B_6	0.342	0.401	2.605	*	*	*
B_7	*	*	*	*	*	*
B_8	*	*	*	*	*	*
			$L/D=0.15$			
Virial Level	ρ_I^*	ρ_N^*	P_N^*	ρ_I^*	ρ_C^*	P_C^*
B_2	1.049	1.206	8.400	4.602	4.733	147.869
B_3	0.420	0.490	3.584	0.807	0.851	19.339
B_4	0.355	0.412	3.263	0.465	0.521	7.181
B_5	0.364	0.417	3.671	*	*	*
B_6	0.405	0.457	4.533	*	*	*
B_7	0.475	0.500	5.770	*	*	*
B_8	0.484	0.504	5.819	0.366	0.374	3.241
			$L/D=0.2$			
Virial level	ρ_I^*	ρ_N^*	P_N^*	ρ_I^*	ρ_C^*	P_C^*
B_2	1.593	1.794	15.828	5.868	5.969	200.885
B_3	0.576	0.660	6.176	1.089	1.148	33.110
B_4	0.466	0.533	5.452	0.600	0.657	11.831
B_5	0.457	0.527	5.909	0.460	0.578	5.995
B_6	0.476	0.544	6.657	*	*	*
B_7	0.495	0.558	7.219	*	*	*
B_8	0.500	0.563	7.246	0.484	0.512	6.572
			$L/D=0.25$			
Virial Level	ρ_I^*	ρ_N^*	P_N^*	ρ_I^*	ρ_C^*	P_C^*
B_2	2.526	2.271	27.818	7.085	7.160	257.573
B_3	0.742	0.841	9.848	1.222	1.262	37.268
B_4	0.572	0.653	8.281	0.701	0.746	15.739
B_5	0.538	0.615	8.463	0.551	0.622	9.134
B_6	0.539	0.615	8.986	*	*	*
B_7	0.541	0.617	9.096	*	*	*
B_8	0.538	0.622	8.825	0.493	0.521	6.540
			$L/D=0.3$			
Virial Level	ρ_I^*	ρ_N^*	P_N^*	ρ_I^*	ρ_C^*	P_C^*
B_2	3.122	3.409	46.997	8.579	8.697	341.763
B_3	0.918	1.021	14.919	1.422	1.454	48.614
B_4	0.676	0.758	11.887	0.807	0.843	21.073
B_5	0.614	0.692	11.504	0.631	0.687	12.647
B_6	0.595	0.674	11.471	0.558	0.645	9.020
B_7	0.585	0.668	11.154	*	*	*
B_8	0.571	0.670	10.370	0.529	0.570	7.719

TABLE II. Approximate phase boundaries as determined by simulation. For the isotropic-nematic, nematic-columnar, and isotropic or cubatic-columnar transitions, the pressure at coexistence and the density of the coexisiting phases is given. For the isotropic or cubatic transition, the ranges of pressure and density within which the transition occurs are given.

		L/D				
Transition		0.1	0.15	0.2	0.25	0.3
Isotropic-nematic	ρ^*	0.351, 0.371	*	*	*	*
	P^*	2.74	*	*	*	*
Isotropic or cubatic	ρ^*	*	0.4–0.57	0.5–0.62	0.52–0.65	0.55–0.67
	P^*	*	3.5–7.0	4.6–9.1	6.6–10.6	8.0–11.9
Nematic-columnar	ρ^*	0.437, 0.482	*	*	*	*
	P^*	4.15	*	*	*	*
Isotropic or cubatic-columnar	ρ^*	*	0.450, 0.546	0.448, 0.542	0.490, 0.612	0.537, 0.655
	P^*	*	4.68	5.43	5.76	6.87

partly due to the more spherical shape of the particles, for which the phase transitions occur at a higher packing fraction, as the virial expansion converges much faster at lower packing fractions. However, as no stable cubatic phase is found at B_6 and B_7 level theory for $L/D=0.15-0.25$, and at the B_7 level for 0.3, it is not possible to say if the predicted coexistence densities are converging at all. The predicted densities at B_8 level theory are somewhat lower than those found from simulations (see Table II), though for $L/D=0.15$ the predicted results are quite close (note that these are the least spherical shaped particles that exhibit cubatic behavior), but without any observed convergence of the virial theory, it is not possible to predict if further virial expansion would give more accurate results. As the particles become more spherical, the predicted equation of state at B_8 level theory for the cubatic phase gets further from the equation of state obtained via simulations, which is to be expected due to the higher packing fractions at which these phases occur.

V. SIMULATION RESULTS

A. $L/D=0.1$

In order to examine the phase behavior, we have performed Monte Carlo compression and expansion runs as described in Sec. II. The resulting equation of state is shown in Fig. 1 and is in good agreement with that of Veerman and Frenkel [9]. Table II lists the location of the phase transitions in the system. The succession of phases observed are illustrated by the snapshots of Fig. 2(b)–2(e). With increasing pressure these are isotropic, nematic, and columnar and solid. This is in agreement with the results of Ref. [9]. However, we also observed a metastable cubatic phase on compression from an isotropic configuration at densities approaching the columnar region of the phase diagram. We shall return to this later.

In addition to viewing snapshots from the simulations, the different phases can be distinguished using the distribution functions introduced in Sec. II A. These have been studied in detail by Veerman and Frenkel [9]. Our purpose here is merely to use them to aid identification of the phases.

The main signature of the nematic phase is in $g_2(r)$ [Fig. 3(a)]. In the isotropic phase, this decays to zero. At higher density, in the nematic phase, the limiting value is finite, reflecting the long-range orientational order. The nematic order parameter is plotted as a function of density in Fig. 4. This clearly shows the isotropic-nematic phase transition. In the 216- and 512-particle systems, nematic order developed spontaneously during the compression runs at a pressure of $P^*\simeq 2.80$. We were unable to observe the formation of a nematic during the 1728-particle compression runs. This is due to the long runs required for equilibration. Instead, Fig. 4 shows the results from the expansion run beginning from a perfect nematic. The order parameter is essentially the same in the nematic phase for all system sizes, but shows typical system-size dependence in the isotropic phase. There is a sharp change in S_{nem} at the phase transition, and from this we locate the coexistence densities at $\rho^*=0.351-0.371$. These are higher than Veerman and Frenkel's values of $\rho^*=0.330-0.335$ [9], but are consistent with the values in Refs. [10,11]. The difference may be due to the fact that our simulations and those in Refs. [10,11] are carried out in the *NPT* ensemble, whereas those in Ref. [9] are carried out in the *NVT* ensemble. Reference [9] also uses a smaller number of particles, but Fig. 4 shows that the system size does not significantly affect the transition density.

In the 216- and 512-particle runs, upon further compression, the system enters the columnar phase at a pressure of $P^*=4.31$. This corresponds to a discontinuity in the equation of state between the densities $\rho^*\simeq 0.437$ and 0.482. Veerman and Frenkel gave the coexistence densities for this transition as $\rho^*=0.497-0.546$ [9]. We have not attempted to locate the transition accurately, but we note that the coexistence densities reported in Ref. [11] are also lower than Veerman and Frenkel's. We can distinguish between the nematic and columnar phases using $g_P(r_\perp)$ [Fig. 3(b)]. In the nematic phase, this is rather featureless, whereas in the columnar phase, there is structure due to the ordering of the columns in the plane.

At higher pressure still, there is a transition to the solid phase. This can be seen in $g(r_\parallel)$ obtained in the expansion

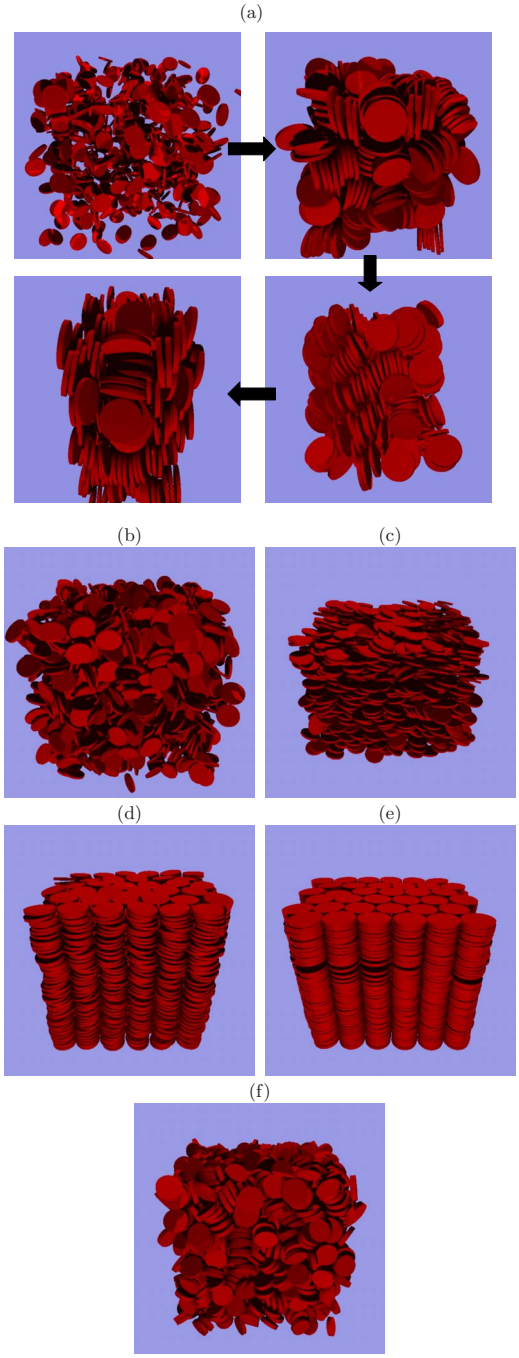

FIG. 2. (Color online) (a) Snapshots during an equilibration run for $L/D=0.1$ and $P^*=5.09$: initial isotropic configuration, after 10^6 Monte Carlo cycles, after 2×10^6 MC cycles, and after 5.8×10^6 MC cycles. (b)–(f) Snapshots illustrating equilibrium structures: (b) isotropic phase ($L/D=0.1$, $P^*=1.17$), (c) nematic phase ($L/D=0.1$, $P^*=3.13$), (d) columnar phase ($L/D=0.1$, $P^*=7.83$), (e) solid phase ($L/D=0.1$, $P^*=31.3$), and (f) cubatic phase ($L/D=0.2$, $P^*=7.29$).

runs from the close-packed solid [Fig. 3(c)]. In the columnar phase, the correlations between particle positions along a column die out within about one particle diameter. In the solid phase, the correlations are long ranged. It is very difficult to give a precise location for this transition, but it is in the vicinity of $\rho^*\simeq0.8$, as also reported in Ref. [9].

It was mentioned earlier that we sometimes obtain a cubatic phase on compression from an isotropic configuration. We first noticed this in an initial compression run for $L/D=0.1$ with 1728 particles. We did not observe a nematic phase as expected, but instead a metastable cubatic phase was observed at densities where the columnar phase might be expected.

In order to establish whether the nematic is stable for this aspect ratio, we have carried out long equilibration runs at two different state points with either an isotropic or a perfect nematic starting configuration. At $P^*=3.52$, from either starting configuration the equilibrium structure is nematic as expected. We repeated the procedure at the higher pressure of $P^*=5.09$, which we expect to be in the columnar phase. In the run starting from the perfect nematic configuration, the particles arranged themselves into columns within 10^6 MC cycles. On the other hand, extremely long runs ($\sim10^7$ MC cycles) are required to equilibrate columnar order starting from an isotropic configuration. The sequence of snapshots in Fig. 2(a) shows the processes occurring. Within 10^6 MC cycles the particles form into short stacks and it appears at this stage as if we have a cubatic phase. It is then a very slow process for these stacks to rotate into the same direction to form a columnar structure. These results show, at least for $L/D=0.1$, that the cubatic is a metastable defective columnar phase, which forms as a transient structure as the system equilibrates.

B. Multiparticle move

The extremely long runs required for equilibration have proved something of a barrier in establishing which phase is thermodynamically stable at a particular state point. One way around this problem might be to implement a multiparticle move to improve sampling. A simple idea due to Jaster [24] is the following. If a particle move causes an overlap, the particle with which it overlaps is also moved, and if this causes an overlap, the next overlapping particle is moved and so on. This continues until there are no further overlaps. If there are two overlaps at any point, the move is rejected. This scheme proved surprisingly effective in equilibrating the nematic phase. Figure 5 compares the evolution of the nematic order parameter during one run in which the multiparticle moves were used and one in which they were not. In terms of the number of Monte Carlo cycles required to reach equilibrium, the improvement is dramatic. Of course, the CPU time per MC cycle will increase, but this turns out to be only by a factor of about 1.5.

For state points in the columnar, the multiparticle moves seem less effective. The moves provide only a marginal improvement in the length of run required to enter the columnar phase from an isotropic initial configuration.

C. $L/D=0.15, 0.2, 0.25, 0.3$

For all other values of the aspect ratio L/D, the following phases were found (from lowest to highest pressure): isotropic, cubatic, and columnar, and solid. This agrees with Veer-

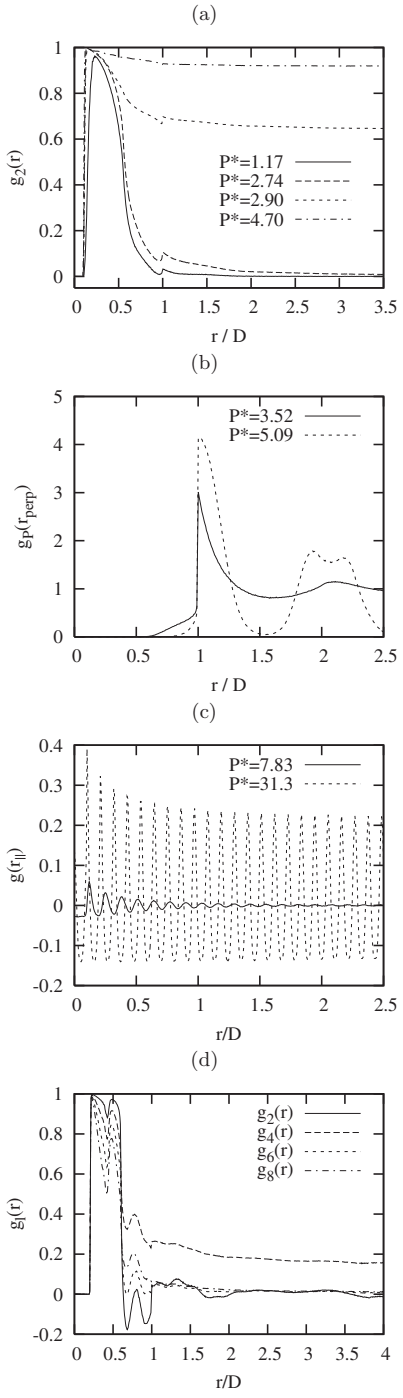

FIG. 3. Pair correlation functions characterizing different phases. (a) $g_2(r)$ for $L/D=0.1$ in the isotropic ($P^*=1.17, 2.74$) and nematic ($P^*=2.90, 4.70$) phases. (b) $g_P(r_\perp)$ for $L/D=0.1$ in the nematic ($P^*=3.52$) and columnar ($P^*=5.09$) phases. (c) $g(r_\parallel)$ for $L/D=0.1$ in the columnar ($P^*=7.83$) and solid ($P^*=31.3$) phases. (d) Orientational correlation functions $g_l(r)$ in the cubatic phase for $L/D=0.2$ at $P^*=7.75$.

man and Frenkel's study [9], in which the cubatic phase was seen at $L/D=0.2$ and 0.3 (although they found the phase to be metastable at $L/D=0.3$). We further observe a cubatic phase at $L/D=0.15$ and 0.25. However, in expansion runs from the crystalline state the cubatic phase was not observed;

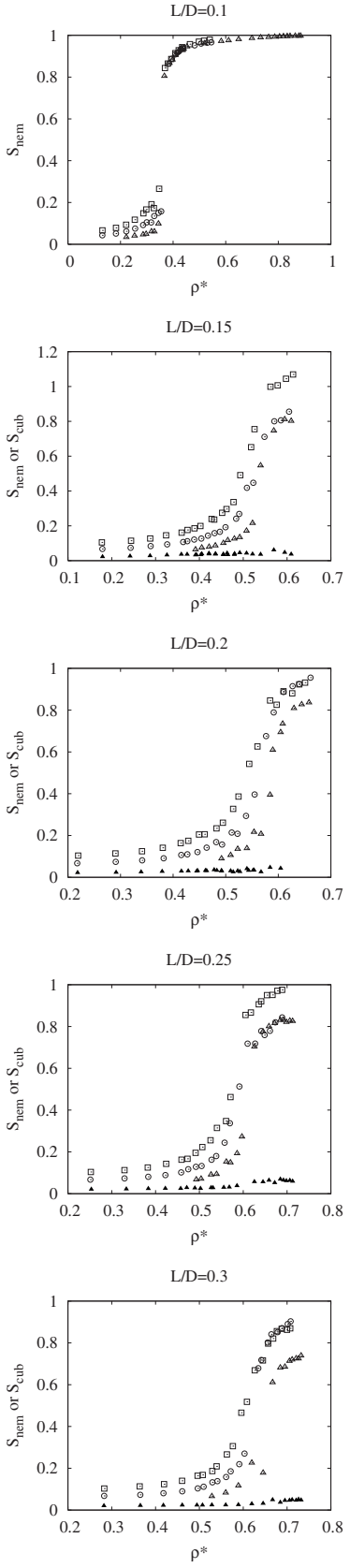

FIG. 4. Nematic and cubatic order parameters as a function of density for different system sizes: 216 particles (squares), 512 particles (circles), and 1728 particles (triangles). For $L/D \geqslant 0.15$ open symbols show S_{cub} and solid symbols show S_{nem}.

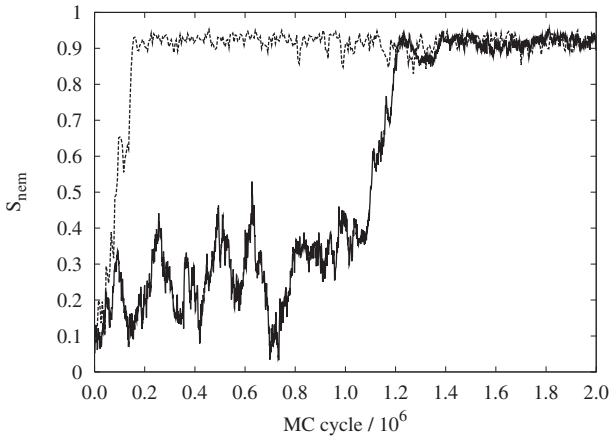

FIG. 5. Nematic order parameter during equilibration runs with (dashed line) or without (solid line) multiparticle moves for a 216 particle system with $L/D=0.1$ at a pressure of $P^*=3.52$.

the system melted directly from the columnar to the isotropic phase at a pressure lower than the isotropic-cubatic transition seen in the compression runs.

The equations of state obtained from the compression and expansion runs are shown in Fig. 1. The equations of state for $L/D=0.2$ and 0.3 are in good agreement with those in Ref. [9]. In Fig. 2(f) we show a snapshot of the cubatic phase, and we can confirm the identification by examining correlation functions. As an example, the orientational correlation functions $g_l(r)$ are shown for a particular state point in the cubatic region in Fig. 3(d). $g_4(r)$ becomes increasingly long ranged with increasing density into the cubatic phase, whereas $g_2(r)$ and $g_6(r)$ decay within two disk diameters. This is due to the cubic symmetry of the cubatic phase. $g_8(r)$ should also decay to a finite value, but at the higher value of l this value may be so small as to be indistinguishable from the noise. The decay of $g_8(r)$ certainly becomes slower as density is increased.

The cubatic and nematic order parameters are plotted as a function of density in Fig. 4. Noting that in the cubatic phase S_{cub} is high, while S_{nem} is low, we can see a transition from the isotropic to the cubatic phase for all four values of L/D. Also apparent is a strong finite-size effect. The transition shifts to higher densities as system size increases.

Unfortunately, the rise of the cubatic order parameter with density across the isotropic-cubatic transition is not very sharp, and Fig. 4 does not provide an accurate estimate of the phase boundary. The best that can be done is to give a range based on this and the hysteresis in the equation of state. These estimates are shown in Table II. For comparison, Veerman and Frenkel [9] give the range $\rho^*=0.54-0.57$ for $L/D=0.2$. Despite the imprecision of these results, it can be seen that the isotropic-cubatic transition shifts to higher density as L/D increases, in accordance with the trend in the theoretical results. The upper bounds of these ranges we have ascribed to the transitions lie within the cubatic-columnar coexistence regions determined from free-energy calculations by Veerman and Frenkel [9]; hence, an isotropic-columnar transition might occur at a density before the transition to the cubatic phase, in which case the cubatic phase would be metastable. Because of the difficulty in locating the phase transitions accurately, we cannot answer this question definitively.

In Table II we also provide estimates for the location of the transition from the isotropic-cubatic branch to the columnar branch. Since we were unable to observe the cubatic phase convert to the columnar during the compression runs, we give as a lower bound for the transition pressure the point at which the columnar converts to isotropic during the expansion runs. The discontinuities in the equations of state corresponding to these lower bounds naturally lie at lower density than the coexistence densities obtained by Veerman and Frenkel ($\rho^*=0.59,0.66$ for $L/D=0.2$ and $\rho^*=0.592,0.689$ for $L/D=0.3$).

Finally, at high pressure is the columnar-solid transition. As for the $L/D=0.1$ case, the main signature of this transition is found in $g(r_{\|})$, but it is difficult to locate with any accuracy. Our results are consistent with Veerman and Frenkel's estimate of $\rho^*\simeq 0.73$ for $L/D=0.2$ [9].

It is clear from both simulation and theory that the cubatic phase is stable over the nematic phase for aspect ratios $L/D\geqslant 0.15$. The stability of the cubatic phase against the columnar phase is not so clear, especially in light of our discovery of a metastable cubatic at $L/D=0.1$. To address this issue, we have carried out equilibration runs for $L/D=0.2$ at state points in the cubatic ($P^*=7.29$) and columnar ($P^*=15.44$) regions of the phase diagram with isotropic or perfect nematic starting configurations. At both state points the results were the same: starting from the nematic configuration, the system becomes columnar and remains there; starting from the isotropic configuration, the system becomes cubatic and remains there. At both state points, in runs up to 6×10^7 MC cycles, there is no sign of the cubatic converting to columnar or vice versa, and hence we cannot draw any conclusions about the relative stability of the two phases.

To obtain a definite answer, one must either find Monte Carlo moves that allow the cubatic and columnar phases to interconvert or else one must be able to accurately determine the free energies of the cubatic and columnar phases and thereby decide which is the most stable. Apart from the previously described multiparticle move due to Jaster, our attempts to find effective Monte Carlo moves include rotations of stacks of particles by 90°, following the ideas given in Refs. [13,28], and also variations of the rejection-free algorithm of Liu and Luijten [29]. To date none of these algorithms have proved successful though we are still exploring other possible cluster moves. We are concurrently conducting free-energy calculations using the expanded-ensemble method and this approach shows signs of promise.

VI. CONCLUSIONS

We have investigated the phase behavior of a system of hard-cut spheres theoretically and by computer simulation. Using a high-order virial theory, a stable nematic phase has been predicted for cut spheres of aspect ratio $L/D=0.1$ and a stable cubatic phase predicted for $L/D=0.15-0.3$, consistent with simulation results. The necessary inclusion of the high-order virials to predict the cubatic phase implies that it is many-body excluded-volume interactions which stabilize the

cubatic phase. Truncation of the virial theory at low order ($<B_5$) will not predict a cubatic phase, so the high-order virials are vital to this theory. Truncation at these low levels gives poor predictions of the transition densities, and truncation at B_6-B_7 gives no predicted transition, due to the negative values of the virial coefficients. At B_8 level theory, reasonable predictions of the equation of state and transition densities are obtained, and the predictions become much more accurate for the less spherical cut spheres, due to the lower packing fractions at which the phase transitions occur for these particles. Overall though, the virial expansion offers an accurate way of predicting stable cubatic phases.

Previous simulation work on this system has covered the aspect ratios $L/D=0.1$, 0.2, and 0.3. Our simulations also include $L/D=0.15$ and 0.25. Since equilibration in some cases requires extremely long runs, we have implemented a multiparticle move due to Jaster [24]. This proved extremely effective in the equilibration of the nematic phase.

We have shown that the nematic phase is stable with respect to the cubatic phase for $L/D=0.1$ and that the opposite is true for $L/D \geqslant 0.15$. This is in accordance with our theoretical results.

We have investigated further the stability of the cubatic phase by performing long runs at particular state points. We have shown that the cubatic phase observed for $L/D=0.1$ in the columnar region of the phase diagram is metastable. On compression from an isotropic configuration, the system initially adopts a cubatic structure. It is only after an extremely long run (of order 10^7 MC cycles) that the short stacks of particles are able to rotate to form a columnar structure. We attempted in the same way to probe the relative stability of the cubatic and columnar phases for $L/D=0.2$. We saw no sign of the cubatic phase converting to columnar or vice versa in runs up to 6×10^7 MC cycles in length. Our results are thus rather inconclusive. We are currently carrying out free-energy calculations using the expanded-ensemble method with the aim of providing a more definitive answer to this question.

[1] D. Frenkel and R. Eppenga, Phys. Rev. Lett. **49**, 1089 (1982).
[2] D. Frenkel, B. M. Mulder, and J. P. McTague, Phys. Rev. Lett. **52**, 287 (1984).
[3] M. A. Bates and G. R. Luckhurst, J. Chem. Phys. **104**, 6696 (1996).
[4] E. Martín del Río, A. Galindo, and E. de Miguel, Phys. Rev. E **72**, 051707 (2005).
[5] D. Caprion, L. Bellier-Castella, and J.-P. Ryckaert, Phys. Rev. E **67**, 041703 (2003).
[6] H. Zewdie, Phys. Rev. E **57**, 1793 (1998).
[7] D. Andrienko, V. Marcon, and K. Kremer, J. Chem. Phys. **125**, 124902 (2006).
[8] O. A. von Lilienfeld and D. Andrienko, J. Chem. Phys. **124**, 054307 (2006).
[9] J. A. C. Veerman and D. Frenkel, Phys. Rev. A **45**, 5632 (1992).
[10] M. M. Piñeiro, A. Galindo, and A. O. Parry, Soft Matter **3**, 768 (2007).
[11] S.-D. Zhang, P. A. Reynolds, and J. S. van Duijneveldt, J. Chem. Phys. **117**, 9947 (2002).
[12] D. van der Beek, T. Schilling, and H. N. W. Lekkerkerker, J. Chem. Phys. **121**, 5423 (2004).
[13] R. Blaak, D. Frenkel, and B. M. Mulder, J. Chem. Phys. **110**, 11652 (1999).
[14] R. Blaak and B. M. Mulder, Phys. Rev. E **58**, 5873 (1998).
[15] R. Blaak, B. M. Mulder, and D. Frenkel, J. Chem. Phys. **120**, 5486 (2004).
[16] B. S. John and F. A. Escobedo, J. Phys. Chem. B **109**, 23008 (2005).
[17] B. S. John, A. Stroock, and F. A. Escobedo, J. Chem. Phys. **120**, 9383 (2004).
[18] A. Chamoux and A. Perera, Phys. Rev. E **58**, 1933 (1998).
[19] A. Donev, J. Burton, F. H. Stillinger, and S. Torquato, Phys. Rev. B **73**, 054109 (2006).
[20] D. A. Triplett and K. A. Fichthorn, Phys. Rev. E **77**, 011707 (2008).
[21] L. Manna, D. J. Milliron, A. Meisel, E. C. Scher, and A. P. Alivisatos, Nature Mater. **2**, 382 (2003).
[22] A. J. Masters, J. Phys.: Condens. Matter **20**, 283102 (2008).
[23] M. A. Bates, M. Dennison, and A. J. Masters, J. Chem. Phys. **129**, 074901 (2008).
[24] A. Jaster, Physica A **264**, 134 (1999).
[25] M. P. Allen, G. T. Evans, D. Frenkel, and B. M. Mulder, Adv. Chem. Phys. **86**, 1 (1993).
[26] F. H. Ree and W. G. Hoover, J. Chem. Phys. **40**, 939 (1964).
[27] M. Dennison, A. J. Masters, D. L. Cheung, and M. P. Allen (unpublished).
[28] M. A. Bates and D. Frenkel, J. Chem. Phys. **112**, 10034 (2000).
[29] J. Liu and E. Luijten, Phys. Rev. Lett. **92**, 035504 (2004).